Formation of back-arc basins by lithospheric warping: examples of the Andaman, Bismarck and Banda Sea basins

Peter Orvoš

Faculty of Natural Sciences, Comenius University in Bratislava, Ilkovicova 6, Bratislava 84215, Slovak Republic, peter.orvos@gmail.com

This is a non-peer reviewed preprint. This manuscript is submitted for publication in Tectonics. Subsequent versions may differ. Feel free to contact me.

Key points: Back-arc basins evolution is accompanied by the subduction retreat, extension and rifting together with arcuate shape of volcanic chains and basin's oval topography

Finite element model shows mechanism how topologically identical structures originate by a thin shell warping

Amphitheatre-like slab geometry of the Andaman, Bismarck and Banda Sea basins resembles pattern of presented deformation

Abstract

Back-arc basins represent an intriguing phenomenon of the lithospheric evolution. They are the places of potential subduction initiation, what makes them highly important features within the theory of plate tectonics. The circumstances of their origin and life cycle are not well understood and whether the retreat of subduction is a cause or consequence of back-arc basin development remains an open issue. In the presented work, a new approach has been used, based on the model of thin shell warping. Within this concept, the plate warps due to proximity of translational boundary when its forward movement is constrained. Following the process, the lithospheric slab can steepen, roll-back and sink to the 660 km transition layer, reaching an amphitheatre-like geometry. The specific shape of deformation resembles the topology of several reference basins. Results show that subduction retreat, back-arc extension and arcuate geometry may only represent different demonstrations of one underlying physical mechanism. Modelling suggests that the movement of plates and their interactions, together with the curvature of the Earth's surface, could be responsible for the formation of back-arc basins.

1. Introduction

The volcanic island arcs, with trenches in front and the basins at their rear, are still puzzling features despite an enormous amount of new data, observations and computer modelling. The question of why they are of arcuate shape has remained largely unresolved. These structures are inherently linked to the subduction of oceanic lithosphere and thus their geometry has been interpreted as its product. It comes from the trivial assumption that sinking slab should adjust to the spherical surface (Frank, 1968). This concept has been challenged by many authors (Schellart and Lister, 2004; Tovish and Gerald, 1978; Mantovani et al., 2001). Despite the indications that

Earth's curvature could nevertheless be the cause of arcuate shapes, no other proposal of such a connection has been given.

Following the observations of Karig (Karig, 1971), occurrence of extension within these regions was explained by motion of the overriding plate away from the subduction front (Hyndman, 1972; Chase, 1978). On the other hand Molnar and Atwater (Molnar and Atwater, 1978) proposed the hinge retreat as a consequence of the lithosphere sinking under its own weight. A compromise between the two cases was the combination of slab hinge migration (or roll-back) with the overriding plate motion (Dewey, 1980). The subduction roll-back became popular due to extensive capabilities of analogous and numerical modelling. If not for two exceptions, the concept of roll-back with hinge retreat would apply to all arc-back-arc systems. But formation of back-arc basins in front of advancing hinges at Izu-Bonin (Miyazaki et al., 2020) and Mariana (Wu et al., 2016) subductions raises concerns about the universality of such a mechanism. Furthermore, the fact that in some cases (Japan Sea Basin, South Fiji Sea Basin) back arc extension came to an end while subduction continued indicates that subduction is not a sufficient condition for back-arc opening.

Another question is what the slab steepening might mean for the back-arc evolution (Mantovani et al., 2001). It is also not clear whether we have enough evidence that trenches migrate at the same speed as volcanic arcs. Therefore, because slab roll-back alone cannot explain either the back-arc basins formation or arc curvature, other processes must be involved. Back-arc systems generally evolve in convergent settings, where shortening occurs along the convex forearc segment and extension at the rear, concave side. Consistent tectonic models should therefore take this under the consideration. The concept with such presumption has become extrusion due to the collision, stressed by several authors (Tapponnier, 1977; Faccenna et al., 1996; Mantovani et al., 2014). But again, extension in the back-arc cannot be solely explained by extrusion (Schellart and Lister, 2004) and mantle upwelling processes must be engaged (Mantovani et al., 2002; Magni et al., 2014). The arcuate shape of trench acquired in these models is as well rather consequence than the cause of back-arc basin formation. Generally, there is little consensus on these issues. Some models assign the decisive role in the origin of back-arc basins to the subduction, while some combine it with extrusion and others view subduction only as a moving boundary. It is then important to ask what is the connection of these phenomena and if subduction is not only the product of the back-arc basins formation.

On this account, young subduction zones connected to marginal basins should be important places to observe these processes. Examples include Philippines and North Sulawesi areas, where there is an evident extension behind subducting lithosphere without volcanic arc presence. It has been proposed by Hall (Hall, 2019) that these are actually new-born subduction zones, originated by thrusting of the marginal lithosphere onto the oceanic one. Structures similar to back-arc subsidence also accompany incipient subduction in the southwest Pacific (Patriat et al., 2019). Other young back-arc basins have also been chosen as examples in the presented conceptual study. Banda Sea, Bismarck Sea and Andaman Sea basins (Fig.1) serve here as a reference for comparison with modelling results. Due to their pronounced arcuate shape and slab geometry they could demonstrate how lithospheric plate deforms itself when constrained in motion by other plates. The reasoning of such approach comes from the effective elastic thickness principles, where the behaviour of lithosphere is approximated by elastically deforming thin shell, downwarped under the action of load. The model presented here replaces static vertical load by a dynamic horizontal load with similar effects and explains these processes on the basis of flexural deformations.

2. Modelling of the shell-related deformations

To investigate the significance of convergence-related processes for back-arc evolution, this study focused on the thin shell deformation. Model configuration should represent the lithospheric plate, approximated by curved viscoelastic layer, variously constrained at the sides (Supporting Information S1). The material of the shell is given properties, commonly utilised for flexure modelling of viscoelastic plates (Tassara et al., 2007). All these properties can be adjusted. Movement of the plate is simulated by axial load applied on one edge of the shell, which is an approach used in the analogue modelling. The dimensions of the plate are 1000x1000 km (1000x1000 mm respectively), two values of thickness have been chosen, 10 and 20 km (10 mm and 20 mm respectively). Thickness of the shell fundamentally influences modelling and it is the most important parameter. With the exception of the central support at the frontal edge, which is stationary, all other parts can move during deformation. Side edges must be constrained against translations diverging from the direction of load. After meshing the model, basic static analysis is run in a solver module. Resulting deformed shell can be further scaled and covered with various contour types. Results are available either as a simple mesh or coloured contours of the membrane force on the surface (Fig. 2). Progress of warping is captured step by step and presented as an animation.

3. Results

3.1. Description of the shell warping processes

During the simulation, unusually complex downwarp develops and deepens quickly, folding the shell in a specific manner (Movie S1). This is because curved layers have a unique capability to transform loads into membrane deformations instead of bending as with flat plates. Therefore the Earth's surface curvature could principally influence behaviour of the deforming lithospheric plate. It is of note that such pronounced vertical deformation develops from a pure horizontal force application and without other initial conditions added.

As a consequence of loading, the shell contracts in length and the wave movement of lateral surfaces folds them down significantly (Fig. 2). The structure is forming into an arcuate shape and even though deformation progresses quickly (Movie S1), its overall topology and horizontal extent changes little. Such character brings potential for downward movements of large magnitude with only a small amount of convergence. The resulting deformation keeps its oval or candle-flame topology visible throughout duration of the whole process (Fig. 3a, b, c). Transformed to lithospheric conditions, the deformation would be situated in the middle part of the lithosphere (oceanic or transient marginal), where properties of the material are suitable to maintain a viscoelastic response. Deformation of shells with about 10 km (10 mm respectively) thickness is the most appropriate to show the nature of described process. One another analysis (20 km thickness) was run to evaluate the results of thickness changes on the shell deformation (Movie S2).

3.2. Visualization of the back-arc geometry

In order to better visualize the arcuate shape of the evolving deformation, a cross-section has been constructed by the horizontal plane. The images in Fig. 3a, b, c represent three snapshots of deformation taken from program animation (Movie S1) combined with an appropriate cut. Its position has been chosen at 100 km isohypse, average depth of the magma production at subduction zones. Spreading of this oval-shaped structure should represent the back-arc outer propagation (Movie S3). Projection of such a cut to the surface level should approximate volcanic arc position (Fig. 3d). This horizontal cross-section visualizes morphology of the back-arc area and final slab position with amphitheatre-like geometry.

4. Discussion

4.1. Comparison of model with the back-arc basins evolution

Extended crust at the continent margins or crustal remnants in the oceans have a transitional character and mechanical properties with effective elastic thickness usually between 10 and 20 km (Watts and Stewart, 1998). Considering the model is mainly geometrical (intended to observe changing topology of the back-arc in 3D), reduction of the lithospheric structure into one viscoelastic layer can be a feasible approximation of the physical reality (Nadai, 1963). Another assumption is that central constraint (support) is stationary in the model. In reality, this boundary moves. But because deformation visual appearance is independent on the load magnitude (it only approximates the plate motion), it does not influence the results to a great extent. It is important to realise, that local plate motion is constrained, not stopped. Therefore deformation, as its part, also moves with plate. The model presents symmetrical development of deformation, which is certainly the ideal scenario. If the back-arc starts from rifting of continental margin, the whole warping structure shifts oceanwards in the direction of lower resistance. Then the trench and volcanic arc develop only at one side. Such example is illustrated in the cross-section (Fig. 4).

Since the yielding of this lithospheric layer is a long-term process, it cannot be suddenly accelerated by an increase in the convergence rate. Changes likely happen on the geological time scale hundreds of thousands of years. This is also the limitation of the model, which provides only relative timing. Warping deformations induce flow in the surrounding mantle they are submerged, what also consumes energy and influences reaction time. As the wave around the warp propagates, it depresses lithosphere into the amphitheatre-like shape, where deep troughs or subduction zones could originate (for example North Sulawesi). This topology is also well visible on matured subduction systems of Banda Sea (Spakman and Hall, 2010) or southern part of Tyrrhenian Sea (Koulakov et al., 2015).

In many cases, supposed delamination accompanies development of the structure. At the beginning, warping mantle lithosphere can separate from the overlying crustal layer. The starting extension then causes the crust beneath originating back-arc basins to be unusually hot (Hall, 2019). As the space further extends, at predisposed zones e.g. former rifts or volcanic arcs lithosphere can tear and divide the basin, usually into two parts. Through these weakened zones melt is able to rise (Fig. 5), filling the gap between the crust of opening basin and delaminated mantle lithosphere. Such process occurs in the incipient stage of the basin evolution. During the next phase with true roll-back, asthenospheric material flows to the rift break and produces a new oceanic crust. Lastly, at final stages, when subducting lithosphere is consumed and opposite continental margin involved, the steepening slab can delaminate again, down-flexing the crust. This mechanism would be part of the explanation why deep troughs originate around some back-arc basins in the late phases of their life (Spakman and Hall, 2010).

4.2. Connection of model to the subduction dynamics

Self-sustained subduction can be initiated, when the lithosphere is sufficiently depressed and starts falling under its own weight. Because the sinking slab from beneath the forming back-arc is delaminated and therefore not hydrated enough (Wu et al., 2021), volcanism likely cannot occur even if the depth over 100 km is reached. Only when steepening induces self-sustained subduction and the slab starts to roll, the oceanic crust is involved, generating enough fluid for melting. The transition can be relatively fast due to both slab steepening (from warping) and subduction. This way an incipient roll-back (in sense of Hall, 2019), resulting from related extension and warping could transform to a true roll-back with fully developed arc volcanism.

Yet one question regarding the volcanism should be answered and that is whether arc advancement is caused by slab steepening or by roll-back. This finding is irrelevant to the arcs life cycle, but would be central to the question of trench migration. If volcanic arc migration is a consequence of the slab steepening, the trench alone can retreat slowly, even remain stationary. Such variant is proposed for the Banda (Spakman and Hall, 2010) or Parece Vela (Wu et al., 2016) back-arcs evolution. Dependence of the arc position on that of the trench, especially in the initial and final stages of back-arc evolution, would be so more complex than we suppose.

5. Conclusions

As this physical mechanism reveals, the lithospheric plate could warp when its movement is impeded and it would allow formation of deep marginal basins of pronounced oval or candle-flame shape. Moreover, the modelling suggests that as little as plate motion and the Earth´s surface curvature would be enough for the origin of these features. Most notable is the topological similarity of the resulting deformation to the observed back-arcs topography patterns. Although providing more examples would help to improve the model's predictions, this attempt is an initial step towards the verification of the observed relationship. Of interest is the ability of this concept to address not only problems of back-arc basins evolution, but also various other connected issues. This way the subduction roll-back, arc migration, tectonic extension and the development of the back-arc basin would become the integral parts of one universal mechanism, which gives this model further potential.

References

Chase, C.G., 1978, Extension behind island arcs and motions relative to hot spots: Journal of Geophysical Research: Solid Earth, v. 83, p. 5385–5387, doi:10.1029/JB083IB11P05385.

Dewey John, F., 1980, Episodicity, sequence, and style at convergent plate boundaries: Special Paper - Geological Association of Canada, v. 20, p. 553–573,

Faccenna, C., Davy, P., Brun, J.-P., Funiciello, R., Giardini, D., Mattei, M., and Nalpas, T., 1996, The dynamics of back-arc extension: an experimental approach to the opening of the Tyrrhenian Sea: Geophysical Journal International, v. 126, p. 781–795, doi:10.1111/J.1365-246X.1996.TB04702.X.

Frank, F.C., 1968, Curvature of Island Arcs: Nature 1968 220:5165, v. 220, p. 363–363, doi:10.1038/220363a0.

Hall, R., 2019, The subduction initiation stage of the Wilson cycle: Geological Society, London, Special Publications, v. 470, p. 415–437, doi:10.1144/SP470.3.

Hyndman, R.D., 1972, Plate motions relative to the deep mantle and the development of subduction zones: Nature, v. 238, p. 263–265, doi:10.1038/238263b0.

Karig, D.E., 1971, Origin and development of marginal basins in the western Pacific: Journal of Geophysical Research, v. 76, p. 2542–2561, doi:10.1029/JB076I011P02542.

Koulakov, I., Jakovlev, A., Zabelina, I., Roure, F., Cloetingh, S., El Khrepy, S., and Al-Arifi, N., 2015, Subduction or delamination beneath the Apennines? Evidence from regional tomography: Solid Earth, v. 6, p. 669–679, doi:10.5194/SE-6-669-2015.

Magni, V., Faccenna, C., Hunen, J. van, and Funiciello, F., 2014, How collision triggers backarc extension: Insight into Mediterranean style of extension from 3-D numerical models: Geology, v. 42, p. 511–514, doi:10.1130/G35446.1.

Mantovani, E. et al., 2014, Generation of back-arc basins as side effect of shortening processes: Examples from the Central Mediterranean: International Journal of Geosciences, v. 5, p. 1062–1079, doi:10.4236/IJG.2014.510091.

Mantovani, E., Albarello, D., Babbucci, D., Tamburelli, C., and Viti, M., 2002, Arc-trench-back arc systems in the Mediterranean area: Examples of extrusion tectonics: Journal of the Virtual Explorer, v. 8, doi:10.3809/JVIRTEX.2002.00050.

Mantovani, E., Vivi, M., Babbucci, D., Tamburelli, C., and Albarell, D., 2001, Back arc extension: Which driving mechanism? Journal of the Virtual Explorer, v. 3, doi:10.3809/JVIRTEX.2001.00025.

Miyazaki, T. et al., 2020, The first 10 Million years of rear-arc magmas following backarc basin formation behind the Izu Arc: Geochemistry, Geophysics, Geosystems, v. 21, p. e2020GC009114, doi:10.1029/2020GC009114.

Molnar, P., and Atwater, T., 1978, Interarc spreading and Cordilleran tectonics as alternates related to the age of subducted oceanic lithosphere: *Earth and Planetary Science Letters*, *v. 41*, p. 330–340, doi:10.1016/0012-821X(78)90187-5.

Nadai, A., 1963, Theory of Flow and Fracture of Solids, vol.2: New York, McGraw-Hill, 470 p.

Patriat, M., Falloon, T., Danyushevsky, L., Collot, J., Jean, M. M., Hoernle, K., et al. (2019). Subduction initiation terranes exposed at the front of a 2 Ma volcanically-active subduction zone. *Earth and Planetary Science Letters*, *508*, 30–40. https://doi.org/10.1016/J.EPSL.2018.12.011

Schellart, W.P., and Lister, G.S., 2004, Tectonic models for the formation of arc-shaped convergent zones and backarc basins: Geological Society of America Special Paper, v. 383, p. 237–258.

Spakman, W., and Hall, R., 2010, Surface deformation and slab–mantle interaction during Banda arc subduction rollback: Nature Geoscience 2010 3:8, v. 3, p. 562–566, doi:10.1038/ngeo917.

Tapponnier, P., 1977, Evolution tectonique du systeme alpin en Mediterranee; poinconnement et ecrasement rigide-plastique: Bulletin de la Société Géologique de France, v. S7-XIX, p. 437–460, doi:10.2113/GSSGFBULL.S7-XIX.3.437.

Tassara, A., Swain, C., Hackney, R., and Kirby, J., 2007, Elastic thickness structure of South America estimated using wavelets and satellite-derived gravity data: Earth and Planetary Science Letters, v. 253, p. 17–36, doi:10.1016/J.EPSL.2006.10.008.

Tovish, A., and Gerald, S., 1978, Island arc curvature, velocity of convergence and angle of subduction: Geophysical Research Letters, v. 5, p. 329–332, doi:10.1029/GL005I005P00329.

Watts, A.B., and Stewart, J., 1998, Gravity anomalies and segmentation of the continental margin offshore West Africa: Earth and Planetary Science Letters, v. 156, p. 239–252, doi:10.1016/S0012-821X(98)00018-1.

Wu, S. et al., 2021, New insights into the structural heterogeneity and geodynamics of the Indo-Burma subduction zone from ambient noise tomography: Earth and Planetary Science Letters, v. 562, doi:10.1016/j.epsl.2021.116856.

Wu, J., Suppe, J., Lu, R., and Kanda, R., 2016, Philippine Sea and East Asian plate tectonics since 52 Ma constrained by new subducted slab reconstruction methods: Journal of Geophysical Research: Solid Earth, v. 121, p. 4670–4741, doi:10.1002/2016JB012923.

Acknowledgements: My thanks go to Miroslav Bielik, Martin Chovan and Jozef Minar for their useful help. I also thank Martina Orvošova for the text corrections.

Author contributions: Peter Orvoš made the models and wrote the text.

Data availability statement: Code and application file used in this study are available from the corresponding author on request. The FEMAP software has been used for modelling. Trial version can be obtained from https://www.plm.automation.siemens.com/store/en-us/trial/femap.html

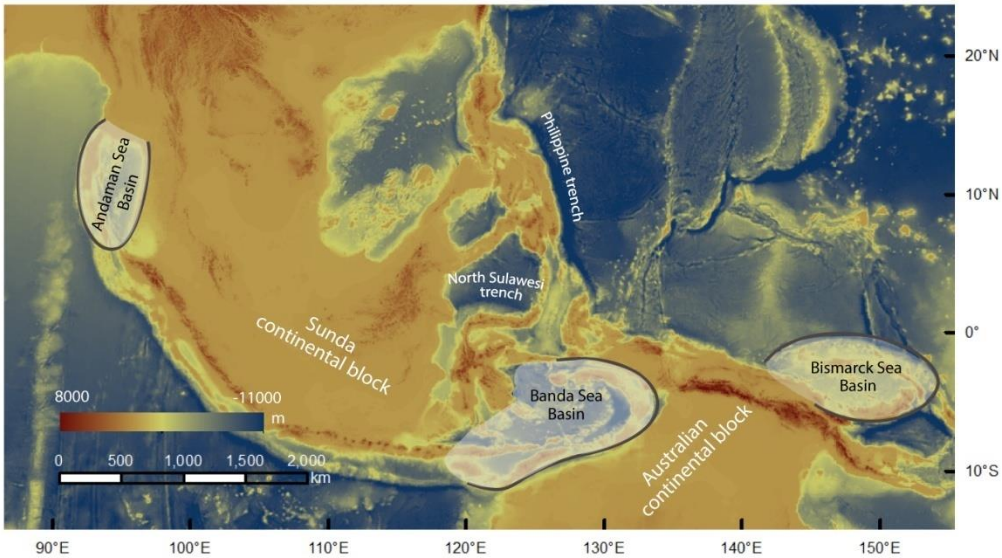

Figure 1. Location map of the reference back-arc basins. Shaded areas show extent and shape of the structures, labelled trenches are considered to be young or incipient.

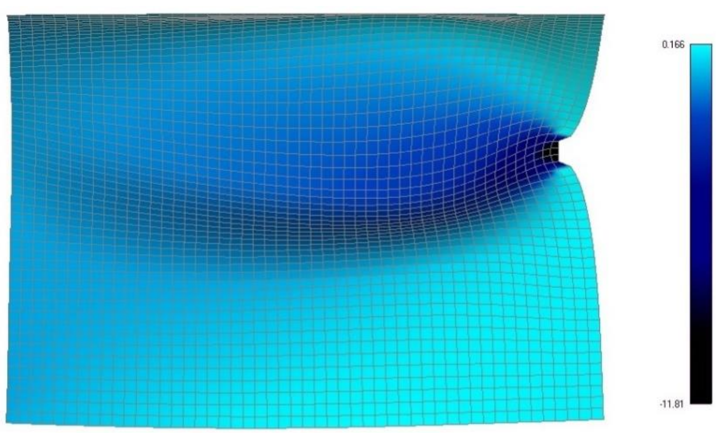

Figure 2. Model of thin shell deformation, 10 mm thickness. Load has been applied on the left edge of the shell (see Supporting Information). Colouring of the model represents continuous contours of membrane force in Nm^{-1}.

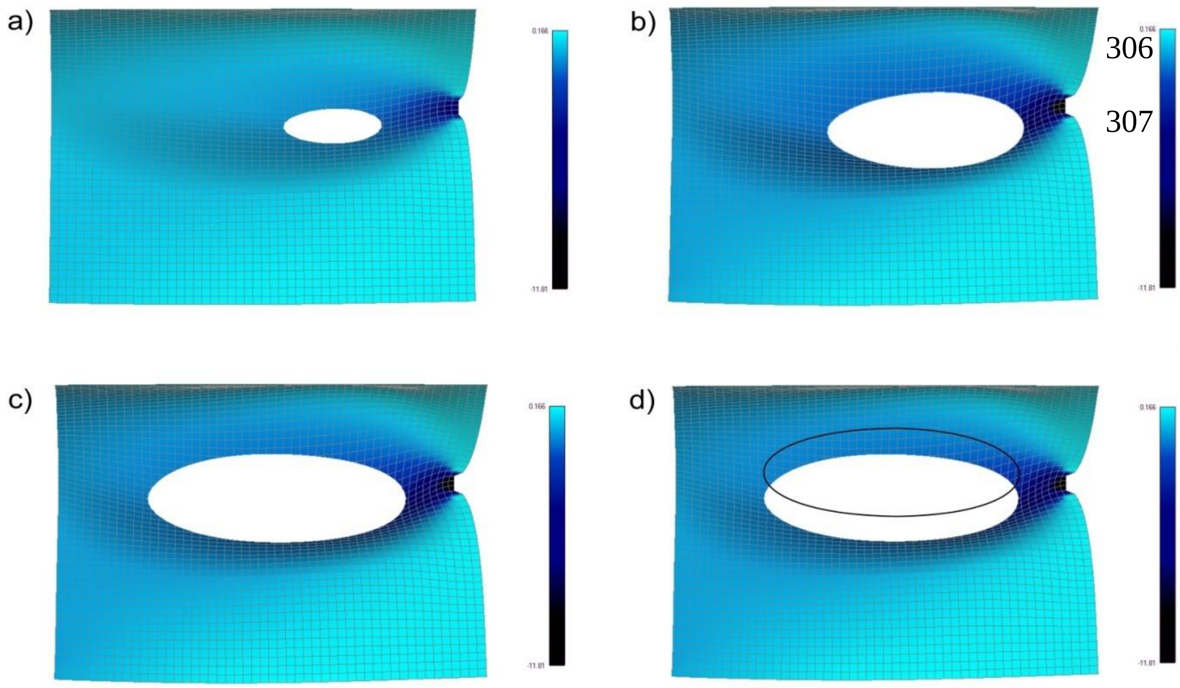

Figure 3. Model of deformation development and back-arc evolution. (a) and (b) show snapshots from model animation in times appr. one third and one half of the whole process duration, (c) is the final state. Horizontal clipping planes are situated at the level of appr. 100 km from the original surface, where melting of the slab causes magma ascent and volcanic arc origin. (d) Projection of melting isohypse visualised by the black ring. Colouring of the model represents continuous contours of membrane force in Nm^{-1}.

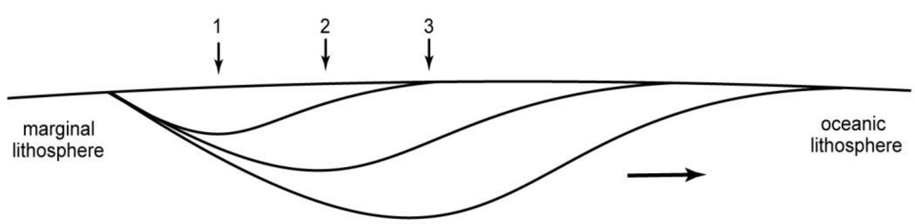

Figure 4. Assymetrical development of the back-arc basin in the cross-section. Sketch is drawn in three phases, numbered vertical arrows mark positions of the basin deepest parts. Horizontal arrow represents direction of the structure's migration.

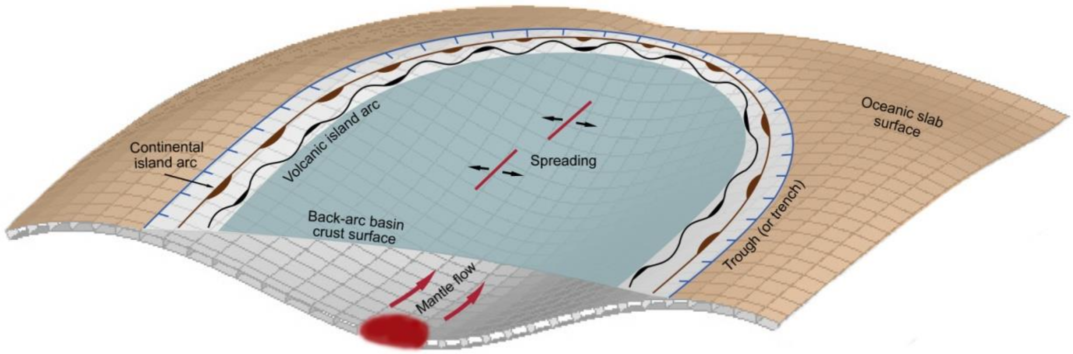

Figure 5. Schematic cartoon showing the model based back-arc basin structure. It is drawn onto the vertical cross section of the model stage, shown in Figure 3b. Arcuate features are situated along the rim, whereas linear create centre of the basin (blue shading). Mantle ascent into the extending space and pressure release cause melting under the spreading centres.

Supporting Information

Construction Of The Thin Shell Finite Element Model

Finite element modelling of the presented problem involves establishing a shell solid of variable thickness, to which appropriate load and constraints are assigned. FEMAP software environment has been utilized to enable fast analysis modifications. Preparation of the model starts from the shell construction. Next, constraints are defined along sides of the body and the governing load. After meshing the shell, analysis is run in the solver module. All modeling operations should be performed in cylindrical coordinates (R, T, Z). The resulting 3D visualization has a wide range of options in scaling, coloring, animation and other post processing. For the purposes of this study, elementary shell surface with medium dimensions has been constructed by revolving a one meter long line. The shell's width is approximately one fifth of the cylinder circumference with narrow (5°) middle segment (Fig. S1). The material of the shell is given the Young's modulus (5×10^{10} Pa) and Poisson's ratio (0.25). For basic analysis, these mechanical parameters are sufficient to define it. Property of the model is chosen as plate element with thickness 10 mm and 20 mm respectively. Subsequently, unit load per length ($1\ Nm^{-1}$) is applied on one side of the shell. Next, establishing the right set of constraints and their configuration has a significant impact on the experiment. Two sides of the model (parallel with load) must be constrained against translation in T direction and also against rotations in R and Z (Fig. S1, label 246 triangles). Other sides (perpendicular to load) are constrained against translation in R (Fig. S1, label 1 triangles), middle segment (the support of the whole model) against all translations and rotations (Fig. S1, label 123 triangles). Meshing of the prepared object takes place with program default settings. Final computing is performed as

Static. Resulting deformed mesh can be further scaled and covered with various contour types to show the specific features of deformation.

Preparation Of Model Outputs For The Process Visualization

The images in Fig. 3a, b, c represent three snapshots of deformation taken from program animation (Movie S1) combined with appropriate cut projections. There are 18 separate steps of animation from the start of the simulated back-arc basin development. The first image is taken approximately in one third of its evolution, second in a half and final in the end, when extension already stopped. Cutting plane is situated in parallel to the original shell surface and approximately in 1/6 of the deformation depth. The outline of the cut is than raised to the surface level, what demonstrates the position of the volcanic arc (black ring in Fig. 3d).

Movie S1 shows deformation of a 10mm thick shell as it progresses in time. One square finite element is of 10x10mm in size. Color scale from the light blue to dark blue represents the increasing membrane force which is the highest in the vicinity of the model support. In that place the high strain persists after the process already slowed significantly. Movie S2 animates a deformation of the shell with 20mm thickness. Movie S3 shows deformation of a 10mm thick shell with horizontal clipping plane as it progresses in time.

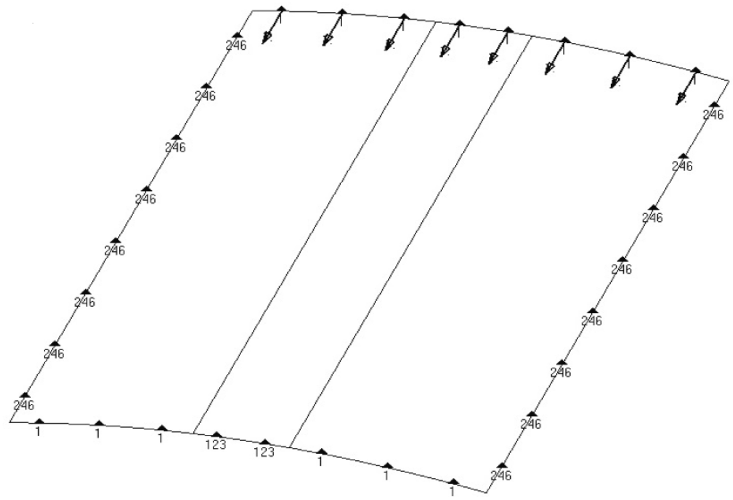

Figure S1. Thin shell construction and modelling variables. Arrows represent applied load, triangles constraints.

Movie S1. Animation of thin shell deformation, 10 mm thickness.

Movie S2. Animation of thin shell deformation, 20 mm thickness.

Movie S3. Animation of thin shell deformation, 10 mm thickness with projected horizontal cutting plane.